B_{s}^{0} lifetime measurement in the CP-odd decay channel B_{s}^{0}→J/ψ f_{0}(980)

V. M. Abazov *et al.* (D0 Collaboration)

B_s^0 lifetime measurement in the CP-odd decay channel $B_s^0 \to J/\psi\ f_0(980)$

V.M. Abazov,[31] B. Abbott,[67] B.S. Acharya,[25] M. Adams,[46] T. Adams,[44] J.P. Agnew,[41] G.D. Alexeev,[31]
G. Alkhazov,[35] A. Alton[a],[56] A. Askew,[44] S. Atkins,[54] K. Augsten,[7] V. Aushev,[38] Y. Aushev,[38] C. Avila,[5]
F. Badaud,[10] L. Bagby,[45] B. Baldin,[45] D.V. Bandurin,[74] S. Banerjee,[25] E. Barberis,[55] P. Baringer,[53] J.F. Bartlett,[45]
U. Bassler,[15] V. Bazterra,[46] A. Bean,[53] M. Begalli,[2] L. Bellantoni,[45] S.B. Beri,[23] G. Bernardi,[14] R. Bernhard,[19]
I. Bertram,[39] M. Besançon,[15] R. Beuselinck,[40] P.C. Bhat,[45] S. Bhatia,[58] V. Bhatnagar,[23] G. Blazey,[47] S. Blessing,[44]
K. Bloom,[59] A. Boehnlein,[45] D. Boline,[64] E.E. Boos,[33] G. Borissov,[39] M. Borysova[l],[38] A. Brandt,[71] O. Brandt,[20]
M. Brochmann,[75] R. Brock,[57] A. Bross,[45] D. Brown,[14] X.B. Bu,[45] M. Buehler,[45] V. Buescher,[21] V. Bunichev,[33]
S. Burdin[b],[39] C.P. Buszello,[37] E. Camacho-Pérez,[28] B.C.K. Casey,[45] H. Castilla-Valdez,[28] S. Caughron,[57]
S. Chakrabarti,[64] K.M. Chan,[51] A. Chandra,[73] E. Chapon,[15] G. Chen,[53] S.W. Cho,[27] S. Choi,[27] B. Choudhary,[24]
S. Cihangir[‡],[45] D. Claes,[59] J. Clutter,[53] M. Cooke[k],[45] W.E. Cooper,[45] M. Corcoran,[73] F. Couderc,[15]
M.-C. Cousinou,[12] J. Cuth,[21] D. Cutts,[70] A. Das,[72] G. Davies,[40] S.J. de Jong,[29, 30] E. De La Cruz-Burelo,[28]
F. Déliot,[15] R. Demina,[63] D. Denisov,[45] S.P. Denisov,[34] S. Desai,[45] C. Deterre[c],[41] K. DeVaughan,[59] H.T. Diehl,[45]
M. Diesburg,[45] P.F. Ding,[41] A. Dominguez,[59] A. Dubey,[24] L.V. Dudko,[33] A. Duperrin,[12] S. Dutt,[23] M. Eads,[47]
D. Edmunds,[57] J. Ellison,[43] V.D. Elvira,[45] Y. Enari,[14] H. Evans,[49] A. Evdokimov,[46] V.N. Evdokimov,[34] A. Fauré,[15]
L. Feng,[47] T. Ferbel,[63] F. Fiedler,[21] F. Filthaut,[29, 30] W. Fisher,[57] H.E. Fisk,[45] M. Fortner,[47] H. Fox,[39] J. Franc,[7]
S. Fuess,[45] P.H. Garbincius,[45] A. Garcia-Bellido,[63] J.A. García-González,[28] V. Gavrilov,[32] W. Geng,[12, 57]
C.E. Gerber,[46] Y. Gershtein,[60] G. Ginther,[45] O. Gogota,[38] G. Golovanov,[31] P.D. Grannis,[64] S. Greder,[16]
H. Greenlee,[45] G. Grenier,[17] Ph. Gris,[10] J.-F. Grivaz,[13] A. Grohsjean[c],[15] S. Grünendahl,[45] M.W. Grünewald,[26]
T. Guillemin,[13] G. Gutierrez,[45] P. Gutierrez,[67] J. Haley,[68] L. Han,[4] K. Harder,[41] A. Harel,[63] J.M. Hauptman,[52]
J. Hays,[40] T. Head,[41] T. Hebbeker,[18] D. Hedin,[47] H. Hegab,[68] A.P. Heinson,[43] U. Heintz,[70] C. Hensel,[1]
I. Heredia-De La Cruz[d],[28] M. Hernández-Villanueva,[28] K. Herner,[45] G. Hesketh[f],[41] M.D. Hildreth,[51] R. Hirosky,[74]
T. Hoang,[44] J.D. Hobbs,[64] B. Hoeneisen,[9] J. Hogan,[73] M. Hohlfeld,[21] J.L. Holzbauer,[58] I. Howley,[71] Z. Hubacek,[7, 15]
V. Hynek,[7] I. Iashvili,[62] Y. Ilchenko,[72] R. Illingworth,[45] A.S. Ito,[45] S. Jabeen[m],[45] M. Jaffré,[13] A. Jayasinghe,[67]
M.S. Jeong,[27] R. Jesik,[40] P. Jiang[‡],[4] K. Johns,[42] E. Johnson,[57] M. Johnson,[45] A. Jonckheere,[45] P. Jonsson,[40]
J. Joshi,[43] A.W. Jung[o],[45] A. Juste,[36] E. Kajfasz,[12] D. Karmanov,[33] I. Katsanos,[59] M. Kaur,[23] R. Kehoe,[72]
S. Kermiche,[12] N. Khalatyan,[45] A. Khanov,[68] A. Kharchilava,[62] Y.N. Kharzheev,[31] I. Kiselevich,[32] J.M. Kohli,[23]
A.V. Kozelov,[34] J. Kraus,[58] A. Kumar,[62] A. Kupco,[8] T. Kurča,[17] V.A. Kuzmin,[33] S. Lammers,[49] P. Lebrun,[17]
H.S. Lee,[27] S.W. Lee,[52] W.M. Lee,[45] X. Lei,[42] J. Lellouch,[14] D. Li,[14] H. Li,[74] L. Li,[43] Q.Z. Li,[45] J.K. Lim,[27]
D. Lincoln,[45] J. Linnemann,[57] V.V. Lipaev[‡],[34] R. Lipton,[45] H. Liu,[72] Y. Liu,[4] A. Lobodenko,[35] M. Lokajicek,[8]
R. Lopes de Sa,[45] R. Luna-Garcia[g],[28] A.L. Lyon,[45] A.K.A. Maciel,[1] R. Madar,[19] R. Magaña-Villalba,[28] S. Malik,[59]
V.L. Malyshev,[31] J. Mansour,[20] J. Martínez-Ortega,[28] R. McCarthy,[64] C.L. McGivern,[41] M.M. Meijer,[29, 30]
A. Melnitchouk,[45] D. Menezes,[47] P.G. Mercadante,[3] M. Merkin,[33] A. Meyer,[18] J. Meyer[i],[20] F. Miconi,[16]
N.K. Mondal,[25] M. Mulhearn,[74] E. Nagy,[12] M. Narain,[70] R. Nayyar,[42] H.A. Neal,[56] J.P. Negret,[5] P. Neustroev,[35]
H.T. Nguyen,[74] T. Nunnemann,[22] J. Orduna,[70] N. Osman,[12] A. Pal,[71] N. Parashar,[50] V. Parihar,[70] S.K. Park,[27]
R. Partridge[e],[70] N. Parua,[49] A. Patwa[j],[65] B. Penning,[40] M. Perfilov,[33] Y. Peters,[41] K. Petridis,[41] G. Petrillo,[63]
P. Pétroff,[13] M.-A. Pleier,[65] V.M. Podstavkov,[45] A.V. Popov,[34] M. Prewitt,[73] D. Price,[41] N. Prokopenko,[34]
J. Qian,[56] A. Quadt,[20] B. Quinn,[58] P.N. Ratoff,[39] I. Razumov,[34] I. Ripp-Baudot,[16] F. Rizatdinova,[68] M. Rominsky,[45]
A. Ross,[39] C. Royon,[8] P. Rubinov,[45] R. Ruchti,[51] G. Sajot,[11] A. Sánchez-Hernández,[28] M.P. Sanders,[22]
A.S. Santos[h],[1] G. Savage,[45] M. Savitskyi,[38] L. Sawyer,[54] T. Scanlon,[40] R.D. Schamberger,[64] Y. Scheglov,[35]
H. Schellman,[69, 48] M. Schott,[21] C. Schwanenberger,[41] R. Schwienhorst,[57] J. Sekaric,[53] H. Severini,[67] E. Shabalina,[20]
V. Shary,[15] S. Shaw,[41] A.A. Shchukin,[34] V. Simak,[7] P. Skubic,[67] P. Slattery,[63] G.R. Snow,[59] J. Snow,[66] S. Snyder,[65]
S. Söldner-Rembold,[41] L. Sonnenschein,[18] K. Soustruznik,[6] J. Stark,[11] N. Stefaniuk,[38] D.A. Stoyanova,[34]
M. Strauss,[67] L. Suter,[41] P. Svoisky,[74] M. Titov,[15] V.V. Tokmenin,[31] Y.-T. Tsai,[63] D. Tsybychev,[64] B. Tuchming,[15]
C. Tully,[61] L. Uvarov,[35] S. Uvarov,[35] S. Uzunyan,[47] R. Van Kooten,[49] W.M. van Leeuwen,[29] N. Varelas,[46]
E.W. Varnes,[42] I.A. Vasilyev,[34] A.Y. Verkheev,[31] L.S. Vertogradov,[31] M. Verzocchi,[45] M. Vesterinen,[41]
D. Vilanova,[15] P. Vokac,[7] H.D. Wahl,[44] M.H.L.S. Wang,[45] J. Warchol,[51] G. Watts,[75] M. Wayne,[51] J. Weichert,[21]
L. Welty-Rieger,[48] M.R.J. Williams[n],[49] G.W. Wilson,[53] M. Wobisch,[54] D.R. Wood,[55] T.R. Wyatt,[41] Y. Xie,[45]
R. Yamada,[45] S. Yang,[4] T. Yasuda,[45] Y.A. Yatsunenko,[31] W. Ye,[64] Z. Ye,[45] H. Yin,[45] K. Yip,[65] S.W. Youn,[45]
J.M. Yu,[56] J. Zennamo,[62] T.G. Zhao,[41] B. Zhou,[56] J. Zhu,[56] M. Zielinski,[63] D. Zieminska,[49] and L. Zivkovic[14]

(The D0 Collaboration[∗])

[1]LAFEX, Centro Brasileiro de Pesquisas Físicas, Rio de Janeiro, RJ 22290, Brazil
[2]Universidade do Estado do Rio de Janeiro, Rio de Janeiro, RJ 20550, Brazil
[3]Universidade Federal do ABC, Santo André, SP 09210, Brazil
[4]University of Science and Technology of China, Hefei 230026, People's Republic of China
[5]Universidad de los Andes, Bogotá, 111711, Colombia
[6]Charles University, Faculty of Mathematics and Physics,
Center for Particle Physics, 116 36 Prague 1, Czech Republic
[7]Czech Technical University in Prague, 116 36 Prague 6, Czech Republic
[8]Institute of Physics, Academy of Sciences of the Czech Republic, 182 21 Prague, Czech Republic
[9]Universidad San Francisco de Quito, Quito, Ecuador
[10]LPC, Université Blaise Pascal, CNRS/IN2P3, Clermont, F-63178 Aubière Cedex, France
[11]LPSC, Université Joseph Fourier Grenoble 1, CNRS/IN2P3,
Institut National Polytechnique de Grenoble, F-38026 Grenoble Cedex, France
[12]CPPM, Aix-Marseille Université, CNRS/IN2P3, F-13288 Marseille Cedex 09, France
[13]LAL, Univ. Paris-Sud, CNRS/IN2P3, Université Paris-Saclay, F-91898 Orsay Cedex, France
[14]LPNHE, Universités Paris VI and VII, CNRS/IN2P3, F-75005 Paris, France
[15]CEA Saclay, Irfu, SPP, F-91191 Gif-Sur-Yvette Cedex, France
[16]IPHC, Université de Strasbourg, CNRS/IN2P3, F-67037 Strasbourg, France
[17]IPNL, Université Lyon 1, CNRS/IN2P3, F-69622 Villeurbanne Cedex,
France and Université de Lyon, F-69361 Lyon CEDEX 07, France
[18]III. Physikalisches Institut A, RWTH Aachen University, 52056 Aachen, Germany
[19]Physikalisches Institut, Universität Freiburg, 79085 Freiburg, Germany
[20]II. Physikalisches Institut, Georg-August-Universität Göttingen, 37073 Göttingen, Germany
[21]Institut für Physik, Universität Mainz, 55099 Mainz, Germany
[22]Ludwig-Maximilians-Universität München, 80539 München, Germany
[23]Panjab University, Chandigarh 160014, India
[24]Delhi University, Delhi-110 007, India
[25]Tata Institute of Fundamental Research, Mumbai-400 005, India
[26]University College Dublin, Dublin 4, Ireland
[27]Korea Detector Laboratory, Korea University, Seoul, 02841, Korea
[28]CINVESTAV, Mexico City 07360, Mexico
[29]Nikhef, Science Park, 1098 XG Amsterdam, the Netherlands
[30]Radboud University Nijmegen, 6525 AJ Nijmegen, the Netherlands
[31]Joint Institute for Nuclear Research, Dubna 141980, Russia
[32]Institute for Theoretical and Experimental Physics, Moscow 117259, Russia
[33]Moscow State University, Moscow 119991, Russia
[34]Institute for High Energy Physics, Protvino, Moscow region 142281, Russia
[35]Petersburg Nuclear Physics Institute, St. Petersburg 188300, Russia
[36]Institució Catalana de Recerca i Estudis Avançats (ICREA) and Institut
de Física d'Altes Energies (IFAE), 08193 Bellaterra (Barcelona), Spain
[37]Uppsala University, 751 05 Uppsala, Sweden
[38]Taras Shevchenko National University of Kyiv, Kiev, 01601, Ukaine
[39]Lancaster University, Lancaster LA1 4YB, United Kingdom
[40]Imperial College London, London SW7 2AZ, United Kingdom
[41]The University of Manchester, Manchester M13 9PL, United Kingdom
[42]University of Arizona, Tucson, Arizona 85721, USA
[43]University of California Riverside, Riverside, California 92521, USA
[44]Florida State University, Tallahassee, Florida 32306, USA
[45]Fermi National Accelerator Laboratory, Batavia, Illinois 60510, USA
[46]University of Illinois at Chicago, Chicago, Illinois 60607, USA
[47]Northern Illinois University, DeKalb, Illinois 60115, USA
[48]Northwestern University, Evanston, Illinois 60208, USA
[49]Indiana University, Bloomington, Indiana 47405, USA
[50]Purdue University Calumet, Hammond, Indiana 46323, USA
[51]University of Notre Dame, Notre Dame, Indiana 46556, USA
[52]Iowa State University, Ames, Iowa 50011, USA
[53]University of Kansas, Lawrence, Kansas 66045, USA
[54]Louisiana Tech University, Ruston, Louisiana 71272, USA
[55]Northeastern University, Boston, Massachusetts 02115, USA
[56]University of Michigan, Ann Arbor, Michigan 48109, USA
[57]Michigan State University, East Lansing, Michigan 48824, USA
[58]University of Mississippi, University, Mississippi 38677, USA

^{59}*University of Nebraska, Lincoln, Nebraska 68588, USA*
^{60}*Rutgers University, Piscataway, New Jersey 08855, USA*
^{61}*Princeton University, Princeton, New Jersey 08544, USA*
^{62}*State University of New York, Buffalo, New York 14260, USA*
^{63}*University of Rochester, Rochester, New York 14627, USA*
^{64}*State University of New York, Stony Brook, New York 11794, USA*
^{65}*Brookhaven National Laboratory, Upton, New York 11973, USA*
^{66}*Langston University, Langston, Oklahoma 73050, USA*
^{67}*University of Oklahoma, Norman, Oklahoma 73019, USA*
^{68}*Oklahoma State University, Stillwater, Oklahoma 74078, USA*
^{69}*Oregon State University, Corvallis, Oregon 97331, USA*
^{70}*Brown University, Providence, Rhode Island 02912, USA*
^{71}*University of Texas, Arlington, Texas 76019, USA*
^{72}*Southern Methodist University, Dallas, Texas 75275, USA*
^{73}*Rice University, Houston, Texas 77005, USA*
^{74}*University of Virginia, Charlottesville, Virginia 22904, USA*
^{75}*University of Washington, Seattle, Washington 98195, USA*
(Dated: June 14, 2016)

The lifetime of the B_s^0 meson is measured in the decay channel $B_s^0 \to J/\psi\ \pi^+\pi^-$ with $880 \leq M_{\pi^+\pi^-} \leq 1080$ MeV/c^2, which is mainly a CP-odd state and dominated by the $f_0(980)$ resonance. In 10.4 fb^{-1} of data collected with the D0 detector in Run II of the Tevatron, the lifetime of the B_s^0 meson is measured to be $\tau(B_s^0) = 1.70 \pm 0.14$ (stat) ± 0.05 (syst) ps. Neglecting CP violation in $B_s^0/\bar{B}_s^0$ mixing, the measurement can be translated into the width of the heavy mass eigenstate of the B_s^0, $\Gamma_H = 0.59 \pm 0.05$ (stat) ± 0.02 (syst) ps^{-1}.

PACS numbers: 14.40.Nd, 13.25.Hw

The B_s^0 and $\bar{B}_s^0$ mesons are produced as flavor eigenstates at hadron colliders, but the particles propagate as mass eigenstates. There are two mass eigenstates, the so-called heavy and light states, which are linear combinations of the flavor eigenstates. In the absence of CP-violation in mixing, the mass eigenstates are also CP eigenstates, with the heavier state expected to be the CP-odd state. The lifetimes of the two mass eigenstates can be different from each other and different from the average B_s^0 lifetime. A measurement of the B_s^0 lifetime in either a pure CP-odd state or pure CP-even state would give important additional information about the B_s^0 system.

The $B_s^0 \to J/\psi f_0(980)$ decay channel corresponds to a pure CP-odd eigenstate decay due to angular momen-

tum conservation, since the parent B_s^0 is spin 0, the $f_0(980)$ has $J^{PC} = 0^{++}$, and the J/ψ has $J^{PC} = 1^{--}$. Throughout this Letter, the appearance of a specific charge state also implies its charge conjugate. This decay channel was first observed by the LHCb collaboration [1], and later confirmed by the Belle [2], CDF [3] and D0 [4] collaborations. A measurement of the B_s^0 lifetime in this channel gives access to the lifetime of the heavy mass eigenstate. The lifetime measurement can be transformed into a measurement of the parameter Γ_H, the decay width of the heavy B_s^0 mass eigenstate. CDF [3] and LHCb [5] have measured this lifetime, reporting $\tau(B_s^0) = (1.70 \pm 0.12 \pm 0.03)$ ps and $\tau(B_s^0) = (1.70 \pm 0.04 \pm 0.026)$ ps respectively, which are in good agreement with each other and somewhat longer than the mean lifetime $\tau(B_s^0) = (1.52 \pm 0.007)$ ps [6].

In this analysis, we report the lifetime of the B_s^0 meson measured in the decay channel $B_s^0 \to J/\psi(\to \mu^+\mu^-)\pi^+\pi^-$ with $880 \leq M_{\pi^+\pi^-} \leq 1080$ MeV/c^2, which is dominated by the $f_0(980)$ resonance and which is CP-odd at the 99% level [7, 8]. The data used in this analysis were collected with the D0 detector during Run II of the Tevatron collider at a center-of-mass energy of 1.96 TeV, and correspond to an integrated luminosity of 10.4 fb^{-1}.

The D0 detector is described in detail elsewhere [9]. The detector components most relevant to this analysis are the central tracking and the muon systems. The former consists of a silicon microstrip tracker (SMT) and a central scintillating fiber tracker (CFT) surrounded by a 2 T superconducting solenoidal magnet. The SMT has a design optimized for tracking and vertexing for pseudo-

---

*with visitors from ^{a}Augustana College, Sioux Falls, SD 57197, USA, ^{b}The University of Liverpool, Liverpool L69 3BX, UK, ^{c}Deutshes Elektronen-Synchrotron (DESY), Notkestrasse 85, Germany, ^{d}CONACyT, M-03940 Mexico City, Mexico, ^{e}SLAC, Menlo Park, CA 94025, USA, ^{f}University College London, London WC1E 6BT, UK, ^{g}Centro de Investigacion en Computacion - IPN, CP 07738 Mexico City, Mexico, ^{h}Universidade Estadual Paulista, São Paulo, SP 01140, Brazil, ^{i}Karlsruher Institut für Technologie (KIT) - Steinbuch Centre for Computing (SCC), D-76128 Karlsruhe, Germany, ^{j}Office of Science, U.S. Department of Energy, Washington, D.C. 20585, USA, ^{k}American Association for the Advancement of Science, Washington, D.C. 20005, USA, ^{l}Kiev Institute for Nuclear Research (KINR), Kyiv 03680, Ukraine, ^{m}University of Maryland, College Park, MD 20742, USA, ^{n}European Orgnaization for Nuclear Research (CERN), CH-1211 Geneva, Switzerland and ^{o}Purdue University, West Lafayette, IN 47907, USA. ‡Deceased.

rapidity of $|\eta| < 3$ [10]. For charged particles, the resolution on the distance of closest approach as provided by the tracking system is approximately 50 μm for tracks with $p_T \approx 1$ GeV/c, where p_T is the component of the momentum perpendicular to the beam axis. It improves asymptotically to 15 μm for tracks with $p_T > 10$ GeV/c. Preshower detectors and electromagnetic and hadronic calorimeters surround the tracker. The muon system is located outside the calorimeter, and consists of multilayer drift chambers and scintillation counters inside 1.8 T iron toroidal magnets, and two similar layers outside the toroids. Muon identification and tracking for $|\eta| < 1$ relies on 10 cm wide drift tubes, while 1 cm minidrift tubes are used for $1 < |\eta| < 2$. We base our data selection on reconstructed charged tracks and identified muons. Events used in this analysis are collected with both single muon and dimuon triggers. To avoid a trigger bias in the lifetime measurement, we reject events that satisfy only impact parameter-based triggers. We simulate signal events with PYTHIA [11] and EvtGen [12], followed by full detector simulation using GEANT3 [13]. To correct for trigger effects, we weight simulated events so that the p_T distributions of the muons match the distributions in data.

The B_s^0 reconstruction begins by reconstructing J/ψ candidates followed by searching for $\pi^+\pi^-$ candidates. To reconstruct $J/\psi \to \mu^+\mu^-$ candidates, events with at least two muons of opposite charge reconstructed in the tracker and the muon system are selected. For at least one of the muons, hits are required in the muon system both inside and outside of the toroids. Both muons must have hits in the SMT and have $p_T > 2.5$ GeV/c. The muon tracks are constrained to originate from a common vertex with a χ^2 probability greater than 1%. Each J/ψ candidate is required to have a p_T greater than 1.5 GeV/c and a mass in the range 2.80–3.35 GeV/c^2.

We require two oppositely charged tracks, assumed to have the pion mass, each with at least two SMT hits and at least two CFT hits, and at least eight total hits in the tracking system. These two tracks are constrained to a common vertex with a χ^2 probability greater than 1%. Each $\pi^+\pi^-$ candidate is required to have a mass in the range $880 \leq M_{\pi^+\pi^-} \leq 1080$ MeV/c^2 and a p_T greater than 1.5 GeV/c. The B_s^0 candidates are reconstructed by performing a constrained fit to a common vertex for the two pions and the two muon tracks, with the latter constrained to the J/ψ mass of 3.097 GeV/c^2 [6]. The B_s^0 candidates are required to have a mass within the range 5.1–5.8 GeV/c^2, and to have a p_T greater than 6.0 GeV/c.

To determine the decay time of the B_s^0, the distance traveled by the candidate projected in a plane transverse to the beam direction is measured, and then a correction for the Lorentz boost is applied. The transverse decay length is defined as $L_{xy} = \boldsymbol{L}_{xy} \cdot \boldsymbol{p}_T / p_T$, where $\boldsymbol{L}_{xy}$ is the vector that points from the primary vertex [14] to the B_s^0

decay vertex, and $\boldsymbol{p}_T$ is the transverse momentum vector of the B_s^0 candidate. The event-by-event value of the proper transverse decay length, λ, for the B_s^0 candidate is given by:

$$\lambda = L_{xy}\frac{cM_B}{p_T}, \tag{1}$$

where M_B is the world average mass value of the B_s^0 meson [6]. In order to remove background, B_s^0 candidates are required to have $\lambda > 0.02$ cm and uncertainties on λ of less than 0.01 cm.

A simultaneous unbinned maximum likelihood fit to the mass and proper decay length distributions is performed to measure the lifetime. The likelihood function $\mathcal{L}$ is defined by:

$$\mathcal{L} = \prod_{j=1}^{N} \left[N_{\text{sig}}\mathcal{F}_{\text{sig}}^j + N_{\text{comb}}\mathcal{F}_{\text{comb}}^j + N_{\text{xf}}\mathcal{F}_{\text{xf}}^j + N_{B^+}\mathcal{F}_{B^+}^j \right], \tag{2}$$

where N is the total number of events and N_{sig}, N_{comb}, N_{xf} and N_{B^+} are the expected number of signal, combinatorial background, cross-feed contamination and $B^\pm \to J/\psi K^\pm$ events in the sample, respectively. All these parameters are determined in the fit. The different background contributions are discussed below.

The functions $\mathcal{F}$ are the product of three probability density functions that model distributions of the mass m, the proper transverse decay length λ, and the uncertainty on the proper decay length σ_λ for the signal, combinatorial background, cross-feed contamination, and $B^\pm$ events

$$\mathcal{F}_\alpha^j = M_\alpha(m_j)T_\alpha(\lambda_j|\sigma_{\lambda_j})E_\alpha(\sigma_{\lambda_j});$$
$$\alpha = \{\text{sig, comb, xf, } B^+\}, \quad (3)$$

where m_j, λ_j, and σ_{λ_j} represent the mass, the transverse proper decay length, and its uncertainty, respectively, for a given event j. The use of the probability density functions T and E follows the method of reference [15]. The specific models and parameters used in the fit are described below.

For the signal, the mass distribution is modeled by a Gaussian function , $M_{\text{sig}}(m_j) = G(m_j; \mu_m, \sigma_m)$, where

$$G(m_j; \mu_m, \sigma_m) = \frac{1}{\sqrt{2\pi}\sigma_m}e^{-(m_j-\mu_m)^2/(2\sigma_m^2)}, \quad (4)$$

with μ_m and σ_m the mean and the width of the Gaussian, determined from the fit.

The combinatorial background is primarily due to random combinations of J/ψ's with additional tracks in the event, and its mass distribution is described by an exponential function

$$M_{\text{comb}}(m_j; a_0) = e^{a_0 m_j}, \tag{5}$$

with a_0 determined from the likelihood fit.

The physics cross-feed contamination is mainly produced by the combination of J/ψ mesons from b hadron decays with other particles produced in the collision, including from the same b hadron. Other b hadron decays with final states such as $B^0 \to J/\psi K\pi$, $B^0 \to J/\psi\pi\pi$ and $B_s^0 \to J/\psi KK$ are reconstructed at mass below the signal of the B_s^0, either due to the lower mass of the B^0 or the incorrect mass assignment of the pion mass to a kaon track. Simulations of these decays show that the cross-feed contamination can be described by a single Gaussian component

$$M_{\mathrm{xf}}(m_j) = G(m_j; \mu_{\mathrm{xf}}, \sigma_{\mathrm{xf}}), \quad (6)$$

where μ_{xf} and σ_{xf} are the mean and the width of the Gaussian, determined from the likelihood fit.

The final contribution arises from $B^\pm \to J/\psi K^\pm$ decays in which the kaon has been assigned a pion mass, and an additional track accidentally forms a vertex with the $J/\psi K^\pm$. The candidate mass is reconstructed in the region of real B_s^0 events. If the higher p_T non-muon track in B_s^0 candidates is assigned a kaon mass, a clear $B^\pm$ signal emerges. Events in this $B^\pm$ mass peak, when interpreted as $J/\psi\pi\pi$, are used as a template [16] to determine the shape of the mass distribution of the $B^\pm \to J/\psi K^\pm$ contamination in the B_s^0 candidates.

The λ distribution for the signal is parameterized by an exponential decay convoluted with a resolution function

$$T_{\mathrm{sig}}(\lambda_j|\sigma_{\lambda_j}) = \frac{1}{\lambda_B} \int_0^\infty G(x; \lambda_j, \sigma_{\lambda_j}) \exp\left(\frac{-x}{\lambda_B}\right) dx, \quad (7)$$

with $\lambda_B = c\tau$ of the B_s^0 to be measured. The λ distribution for the background components is parametrized by the sum of two exponential decay functions modeling combinatorial background $T_{\mathrm{comb}}(\lambda_j)$, an exponential decay for the cross-feed contamination $T_{\mathrm{xf}}(\lambda_j)$, and an exponential decay function that describes $T_{B+}(\lambda_j)$ for $B^\pm$ contamination.

The distribution of the λ uncertainty $E_{\mathrm{sig}}(\sigma_{\lambda_j})$ is described by a phenomenological model, using an exponential with decay constant $1/\zeta$, convoluted with a Gaussian with mean ϵ and width δ:

$$E_{\mathrm{sig}}(\sigma_{\lambda_j}; \zeta, \epsilon, \delta) = \frac{1}{\zeta} e^{-\sigma_{\lambda_j}/\zeta} \otimes G(\sigma_{\lambda_j}; \epsilon, \delta), \quad (8)$$

where the parameters ζ, ϵ and width δ are determined from the fit in the sample of events. The uncertainties in λ for the background components are treated in the same manner.

The fit yields $c\tau(B_s^0) = 504 \pm 42$ μm and the numbers of signal decays to be 494 ± 85. Figure 1 shows the mass, λ and λ uncertainty distributions for data with the fit results superimposed. Figure 2 shows the $M(\pi^+\pi^-)$ mass distribution for events with $M(\mu^+\mu^-\pi^+\pi^-)$ within one
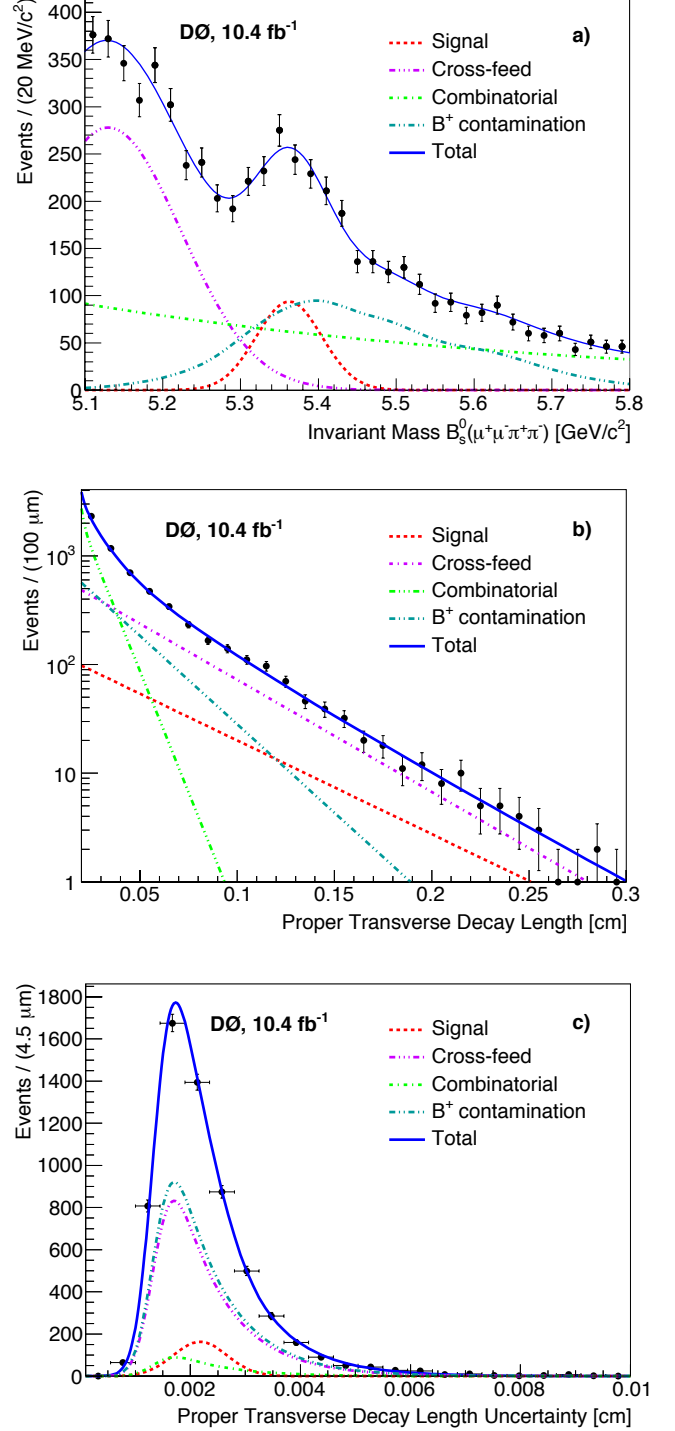

FIG. 1: Distributions of (a) invariant mass, (b) proper transverse decay length, and (c) proper transverse decay length uncertainty for B_s^0 candidates, with the fit results superimposed. Each of the different background components is indicated in the figure. The fit yields $c\tau(B_s^0) = 504 \pm 42$ μm.
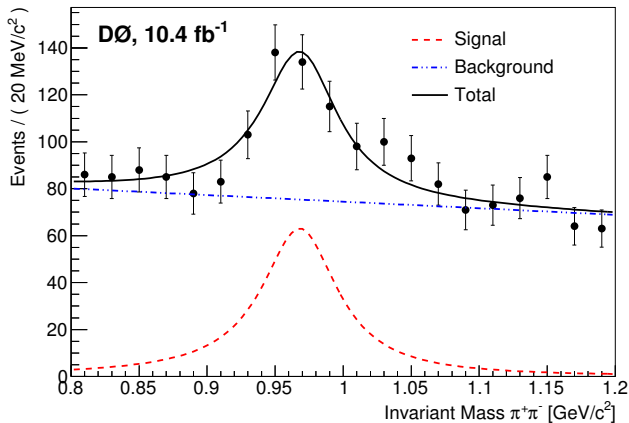
FIG. 2: $M(\pi^+\pi^-)$ distribution for events with $M(\mu^+\mu^-\pi^+\pi^-)$ within $\pm 1\sigma$ of the B_s^0 mass.

TABLE I: Summary of systematic uncertainties in the B_s^0 lifetime measurement. The total uncertainty is determined by combining individual uncertainties in quadrature.

Source	Variation (μm)
Alignment	5.4
$\pi^+\pi^-$ invariant mass window	8.0
Fit bias	4.4
Distribution models	12.5
Total	16.4

σ of the B_s^0 mass. The $M(\pi^+\pi^-)$ distribution is fit with a Flatté function [17–19] and a polynomial background.

Table I summarizes the systematic uncertainties considered for this measurement. The contribution from possible misalignment of the SMT detector has been previously determined to be 5.4 μm [20]. The invariant mass window used for the $\pi^+\pi^-$ distribution is varied from its nominal value of 200 MeV/c^2 to 160 and 240 MeV/c^2 and the fit is performed for each new mass window selection. This results in a systematic uncertainty of 8 μm. We test the modeling and fitting method used to estimate the lifetime using data generated in pseudoexperiments with a range of lifetimes from 300 to 800 μm. A bias arises due to imperfect separation of signal and background. Since the background has a shorter lifetime than the signal, the result is a slight underestimate of the signal lifetime. The bias has a value of -4.4 μm for an input lifetime of 500 μm and 500 signal events. We have corrected the lifetime for this bias and a 100% uncertainty on the correction has been applied to the result. We estimate the systematic uncertainty due to the models for the λ and mass distributions by varying the parameterizations of the different components: (i) the cross-feed contamination is modeled by two Gaussian functions instead of one, (ii) the exponential mass distribution for the combinatorial background model is replaced by a first order polynomial, (iii) the smoothing of the non-parametric function that models the $B^\pm$ contamination is varied, and (iv) the exponential functions modelling the background λ distributions are smeared with a Gaussian resolution similar to the signal. To take into account correlations between the effects of the different models, a fit that combines all different model changes is performed. We quote the difference between the result of this fit and the nominal fit as the systematic uncertainty.

Several cross-checks of the lifetime measurement are performed. The mass windows are varied, the recon-

structed B_s^0 mass is used instead of the world average [6] value, and the data sample is split into different regions of pseudorapidity and of azimuthal angle. All results obtained with these variations are consistent with the nominal measurement. Using the $B^\pm$ background sample extracted from the data, we performed a fit for the lifetime of this component of the background. The result is in good agreement with the values obtained from the global fit. We have also fit the lifetime of the cross-feed contamination from the simulation and again good agreement with the global fit is observed.

In order to estimate the effect of a small non CP-odd component in the analysis, we performed the fit with two exponential decay components for the signal, with the lifetime of one of them fixed to the world average of the CP-even B_s^0 lifetime [6], and its fraction to be 0.01 as found by the LHCb experiment [5]. The lifetime fit finds a variation of 1 μm with respect to the nominal fit result.

In summary, the lifetime of the B_s^0 is measured to be:

$$c\tau(B_s^0) = 508 \pm 42 \text{ (stat)} \pm 16 \text{ (syst)} \ \mu\text{m}, \qquad (9)$$

from which we determine:

$$\tau(B_s^0) = 1.70 \pm 0.14 \text{ (stat)} \pm 0.05 \text{ (syst)} \text{ ps}, \qquad (10)$$

in the decay channel $B_s^0 \to J/\psi\pi^+\pi^-$ with $880 \leq M_{\pi^+\pi^-} \leq 1080$ MeV/c^2. In the absence of CP violation in mixing, this measurement can be translated into the width of the heavy mass eigenstate of the B_s^0:

$$\Gamma_H = 0.59 \pm 0.05 \text{ (stat)} \pm 0.02 \text{ (syst)} \text{ ps}^{-1}. \qquad (11)$$

This result is in good agreement with previous measurements and provides an independent confirmation of the longer lifetime for the CP-odd eigenstate of the $B_s^0/\bar{B}_s^0$ system.

---

[1] R. Aaij *et al.* (LHCb Collaboration), *First observation of $B_s^0 \to J/\psi f_0(980)$ decays*, Phys. Lett. B **698**, 115 (2011).

[2] J. Li *et al.* (Belle Collaboration), *Observation of $B_s^0 \to J/\psi f_0(980)$ and Evidence for $B_s^0 \to J/\psi f_0(1370)$*, Phys. Rev. Lett. **106**, 121802 (2011).

[3] T. Aaltonen *et al.* (CDF Collaboration), *Measurement of branching ratio and B_s^0 lifetime in the decay $B_s^0 \to J/\psi f_0(980)$ at CDF*, Phys. Rev. D **84**, 052012 (2011).

[4] V.M. Abazov *et al.* (D0 Collaboration), *Measurement of the relative branching ratio of $B_s^0 \to J/\psi f_0(980)$ to $B_s^0 \to J/\psi \phi$*, Phys. Rev. D **85**, 011103(R) (2012).

[5] R. Aaij *et al.* (LHCb Collaboration), *Measurement of the $\bar{B}_s^0$ Effective Lifetime in the $J/\psi f_0(980)$ Final State*, Phys. Rev. Lett. **109**, 152002 (2012)

[6] K. A. Olive *et al.* (Particle Data Group), *Review of Particle Physics*, Chin. Phys. C **38**, 090001 (2014).

[7] R. Aaij et al. (LHCb Collaboration), *Analysis of the resonant components in $\bar{B}_s^0 \to J/\psi \pi^+ \pi^-$*, Phys. Rev. D **86**, 052006 (2012).

[8] R. Aaij et al. (LHCb Collaboration), *Measurement of resonant and CP components in $\bar{B}_s^0 \to J/\psi \pi^+ \pi^-$ decays*, Phys. Rev. D **89**, 092006 (2014).

[9] V.M. Abazov *et al.*, *The upgraded D0 detector*, Nucl. Instrum. Methods A **565**, 463 (2006).

[10] $\eta = -\ln[\tan(\theta/2)]$, where θ is the polar angle with respect to the beamline.

[11] T. Sjöstrand, S. Mrenna and P.Z. Skands, *PYTHIA 6.4 Physics and Manual*, J. High Energy Phys. **05**, 026 (2006)

[12] D.G. Lange, *The EvtGen particle decay simulation package*, Nucl. Instrum. Methods in Phys. Res. A **462**, 152 (2001); for details see `http://www.slac.stanford.edu/~lange/EvtGen`.

[13] R. Brun *et al.*, *GEANT detector description and simulation tool*, CERN program library long writeup W, **5013**, (1993).

[14] The primary vertex of the $p\bar{p}$ interaction is determined for each event using the average transverse position of the beam-collision point as a constraint.

[15] G. Punzi, *Comments on Likelihood fits with variable resolution*, arXiv physics/0401045 (2004).

[16] K. Cranmer, *Kernel estimation in high-energy physics*, Comput. Phys. Comm. **136**, 3 (2001).

[17] J.B. Gay *et al.*, *Production and decay properties of the $\delta(970)$ meson*, Phys. Lett. B **63**, 220 (1976).

[18] S. M. Flatté, *Coupled-channel analysis of the $\pi\eta$ and $K\bar{K}$ systems near $K\bar{K}$ threshold*, Phys. Lett. B **63**, 224 (1976).

[19] S. M. Flatté, *On the nature of 0+ mesons*, Phys. Lett. B **63**, 228 (1976).

[20] V.M. Abazov *et al.*, *Measurement of the Λ_b^0 Lifetime in the Decay $\Lambda_b^0 \to J/\psi \Lambda^0$ with the D0 Detector*, Phys. Rev. Lett. **94**, 102001 (2005).